# Titanium Anodization Efficiency Through Live Gravimetric Measurement of Oxygen Evolution

Davide Prando
Politecnico di Milano
Via Mancinelli 7
Milan, 20135
Italy

MariaPia Pedeferri
Politecnico di Milano
Via Mancinelli 7
Milan, 20135
Italy

Santiago Fajardo
National Centre for Metallurgical Research
(CENIM-CSIC)
Avda. Gregorio del Amo 8
Madrid, 28040
Spain

Marco Ormellese
Politecnico di Milano
Via Mancinelli 7
Milan, 20135
Italy

Maria Vittoria Diamanti
Politecnico di Milano
Via Mancinelli 7
Milan, 20135
Italy

## ABSTRACT

Anodization is an easy and reliable treatment to improve titanium corrosion resistance in severe environments. In previous studies its effectiveness in enhancing oxide film resistance in halides was correlated with anodization cell voltage. To increase treatment industrial applicability, energy efficiency has to be maximized. For this purpose, a gravimetric approach was applied to study oxygen evolution during titanium anodic oxidation. Anodization efficiencies, calculated from on-line $O_2$ evolution measurement, were used to determine the most efficient galvanostatic anodization treatment by comparing different anodic current densities, from 1 to 20 mA/cm$^2$, and different electrolytes ($H_2SO_4$ - $K_2SO_4$). Anodization cell voltages were correlated with oxide thickness through indirect spectrophotometric measurements to compare the amount of charge needed to reach a certain film thickness in different anodization conditions.

Key words: anodization, efficiency, oxygen evolution, surface treatment, titanium.

## INTRODUCTION

Titanium and its alloys are worldwide appreciated for their superior corrosion resistance. This resistance is due to a thin (1.5 nm - 10 nm)[1] but compact and chemically stable oxide layer that is naturally formed when the metal is exposed to the air. For this property, together with high strength, low density and high fracture toughness[2,3], they are applied in critical environments where even high-end stainless steels are not suitable (duplex UNS S31803 and UNS S32750 in concentrated chlorides solution[4,5]). The application fields requiring titanium for its corrosion resistance range from offshore plants, acid environment, aerospace[6,7], automotive, high temperature, chemical and food industry[8–10], marine hydrometallurgical application and even nuclear fuel wastes containment[1,11–14].

In such aggressive environments, even titanium may suffer different form of corrosion[15,16]. The most critical of them are due to localized breaking of passive layer and this is favored by the presence of concentrated halides, such hot salty water (above 200 °C) or bromide containing species[17,18]. To further improve titanium corrosion resistance in these environments, specific treatments can be employed. Corrosion resistance enhancing treatments can be divided in two families: chemical composition changing treatments and oxide thickening treatments. The first family includes alloying with other elements (mainly Pd, Mo and Ni)[19], nitration[20,21], vacuum plasma spray coating, plasma spray coating and chemical vapor deposition[22]. Treatments of the second family relies on the possibility to thicken the naturally formed $TiO_2$ film with an external electrical, chemical or thermal driving force, using respectively anodic, chemical or thermal oxidation. Among them, anodization is the easiest, more reliable and precisely controllable.[23] However, industrial application requires balance power consumption with productivity. In this scenario it is vital to proceed in the most efficient way.

Anodization efficiency is defined as the amount of charge devoted to oxide formation against total charge supplied to the system (Eq. I).

$$(Q_{tot} - Q_{O_2})/Q_{tot} = Q_{film} / Q_{tot} \quad \text{(I)}$$

The charge supplied to the system is divided in two main reactions:

$$Ti \rightarrow Ti^{4+} + 4e^- \quad \text{(II)}$$

$$2H_2O \rightarrow O_2 + 4H^+ + 4e^- \quad \text{(III)}$$

Titanium oxidation (Eq. II) is hindered by parasitic oxidation reactions. Usually anodization bath is properly chosen to prevent parasitic reaction other than water oxidation (Eq. III).

Assuming unitary efficiency, it is possible to calculate titanium dioxide film thickness from electrical charge supplied to the system. As titanium is water insoluble, the amount of titanium dioxide is calculated with Faraday eq. (Eq. IV).

$$n = Q / ZF \quad \text{(IV)}$$

With *n* number of moles reacted, *Q* total charge associated with charge carriers in solution, *Z* number of electrons transferred per ions and *F* faraday constant. As $TiO_2$ density, obtained by RBS and optical measurements, is 3.7 g/cm$^3$, 1 C/cm$^2$ would correspond to 559 nm film in absence of any parasitic reaction. [24]

This calculation is used to obtain anodization efficiency in indirect way, by measuring oxide thickness, knowing the amount of charge circulated, it is possible to compare the theoretical oxide thickness in absence of any parasitic reaction with the real one, obtaining anodization efficiency[25]. With a more sophisticated approach it is possible to directly measure process efficiency. The amount of oxygen evolved from the anode during titanium anodic oxidation is measured by a graduated cylinder put upside-down in the electrolyte above the anode. Evolved gas is collected in the cylinder, then its

volume is then converted in amount of charge used for water oxidation reaction[26]. This method, although more accurate than the indirect one, suffers some limitations:

- The minimum amount of evolved oxygen is limited by optical detection in the cylinder
- Measure resolution is limited by graduated cylinder resolution
- Oxygen evolved from anode surface needs to physically detach from the surface and migrate into the cylinder to be detected
- Live measurement is very difficult, this means that only one measure per experiment can be obtained

To overcome these problems another procedure, based on gravimetric measurements, can be applied. This method, introduced by M. Curioni et al.[27], consist in using a balance to record weight difference of a beaker placed upside-down over the anode. This setup is described in par. Gravimetric test setup.

The aim of this study is to use gravimetric approach, already used on aluminum anodization[28], to obtain a live measurement of titanium anodization efficiency. Then compare the effect of different current densities and different anodization electrolyte to optimize the efficiency of anodic oxidation treatments in order to increase its industrial applicability.

## MATERIAL AND METHODS

### Sample preparation

Square samples 20 x 20 x 1.6mm were obtain by cold-cut from titanium UNS R50400 (ASTM grade 2) sheet. After manual polishing with 800 grit SiC paper in two perpendicular directions, each sample was degreased in EtOH and soldered on the back to an electrical wire. Then, the whole sample except the non-soldered face was cold mounted in epoxy-resin in order to keep the possibility to polarize the sample when fully immersed in the electrolyte, without exposing any other metal to the bath.

### Gravimetric test setup

Oxygen evolution was measured during galvanostatic anodization. Measurements were carried out in a conventional two-electrodes cell (800 ml,) with a Pt counter-electrode, at 5 - 10 - 15 and 20 $mA/cm^2$. Tests were performed in $H_2SO_4$ 0.5 M and at 10 $mA/cm^2$ in $K_2SO_4$ 0.5 M. Anodic oxidations were stopped when cell voltage reached 120 V in all cases except 5 $mA/cm^2$ where low current density did not allow to reach that voltage in reasonable times, in that case, 100 V was taken as limit value. The current was supplied by an AimTTi[†] PLH120 DC power supply, able to operate up to 120 V and 0.75 A.

To investigate early stages of anodization with more control on supplied current and cell voltage reached, a potentiostat Gamry[†] Instruments Interface 1000E was used in galvanostatic experiment at 1 $mA/cm^2$ up to 12 V in $H_2SO_4$ 0.5 M.

All the experiments were repeated minimum two times to ensure repeatability.

Room temperature was kept between 23 °C and 25 °C, the exact temperature was recorded prior of each experiment for oxygen volume/moles conversion.

Solutions pH was measured before and after anodizing experiments by using a Crison[†] GLP22 pH meter. $H_2SO_4$ pH was 0.5 without any substantial change after all the performed anodizations. $K_2SO_4$ pH was 5.3, unaffected by the 4 anodizations made in this electrolyte.

---

[†] Trade name

Gravimetric oxygen evolution measurement setup is schematized in Fig. 1.

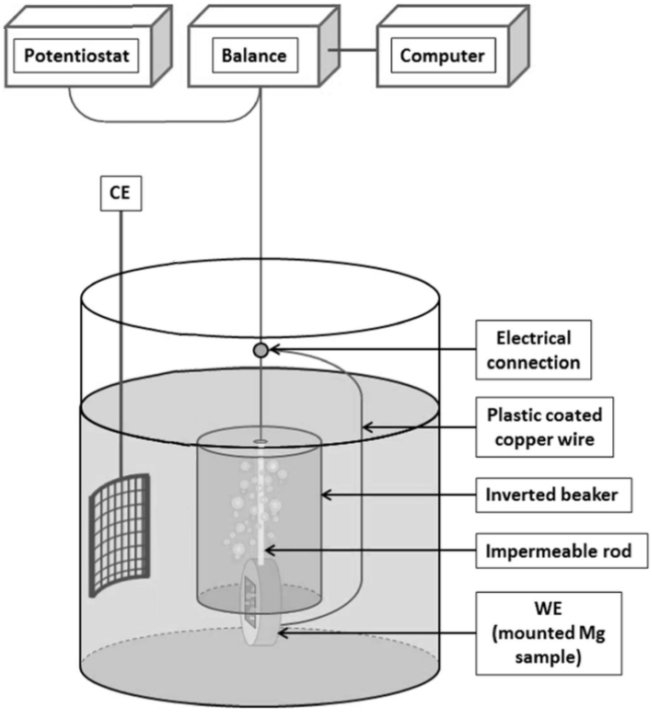


**Figure 1: Schematic of the experimental gravimetric setup for oxygen evolution from mounted titanium sample subject to anodic polarization.[29]**

An inverted beaker, made of glass to avoid gas permeation, was attached to a wire hanging from the bottom of a Mettler Toledo[†] balance (model MS204S) with an accuracy of $10^{-4}$ g. Titanium sample was inserted in the beaker, where all the oxygen produced at anode surface was collected, causing a decreasing in recorded weight. Weight difference is associated with volume of electrolyte displaced by evolved oxygen and can be translated in current density associated with this parasitic reaction.

Setup resolution

Setup resolution can be calculated as follow: $\rho_{H_2SO_4} 0.5\ M = 1.022 g/cm^3$

Barometric pressure during first experiment: 101300 Pa

Temperature during first experiment: 23.6 °C

Oxygen evolution rate responsible of 0. mg/s (balance resolution) of weight decrease rate correspond to:

$$\frac{\frac{10^{-4}\ g}{1.022\ g/cm^3} \cdot 10^{-6}\ \frac{m^3}{cm^3} \cdot 101300\ Pa}{8.3144\ \frac{J}{K} mol \cdot 296.6\ K} = 4.019 \cdot 10^{-9}\ mol \qquad \text{(V)}$$

[†] Trade name

That, using Faraday eq., corresponds to: $4.019 \cdot 10^{-9} \cdot 2 \cdot 96500 = 7.757 \cdot 10^{-4}$ A. This is the minimum current density associated with oxygen evolution detectable by this experimental setup.

As beaker is immersed under electrolyte free surface, gas pressure inside the beaker differs from barometric pressure. Fajardo and Frankel [29] already considered this difference and; being in the order of $10^{-}$ atm, it may be neglected.

**Film thickness measurement**

Described setup allows not only to record oxygen evolved from the anode at the end of an experiment, but a live measurement during anodization. Thus, efficiency can be monitored not only in function of time, but also in function of cell voltage reached at a certain time. However, efficiencies of anodic oxidation in different electrolytes have to be compared in function of oxide thickness achieved, and not in function the cell voltage reached because anodizing bath might have an influence on the relation cell voltage/oxide thickness.

To compare results obtained in $H_2SO_4$ 0.5 M and $K_2SO_4$ 0.5 M, anodizations were repeated and stopped at cell voltages of 5 - 10 - 15 - 20 - 25 - 30 - 35 - 40 - 50 - 60 - 70 - 80 - 90 and 100 V. Values above 100 V were discarded as anodic spark deposition introduces important deviation in oxide growth linearity. Oxide thicknesses were measured by indirect spectrophotometric analyses using a Konica-Minolta spectrophotometer CM-2500d.

## RESULTS

**Anodization kinetic**

Cell voltage growth during galvanostatic anodization in $H_2SO_4$ 0.5 M and $K_2SO_4$ 0.5 M at current densities from 5 to 20 mA/cm$^2$ is shown in Fig. 2.

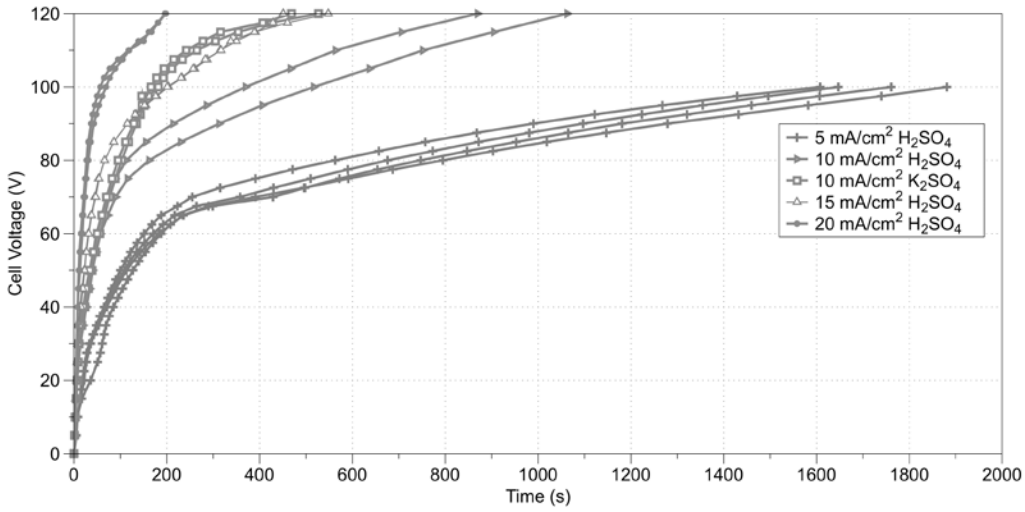


**Figure 2: Cell voltage growth kinetic during galvanostatic anodization in $H_2SO_4$ and $K_2SO_4$ at different current density.**

As expected, using the same electrolyte, higher current density leads to faster anodization. Moreover, increasing current density increases voltage range in which voltage growth deviates from linearity: from around 60 – 70 V at 5 mA/cm$^2$ to 100 - 110 V at 20 mA/cm$^2$.

It is also important to notice that using different electrolytes leads to different anodization kinetics. Potassium sulphate 0.5 M showed faster voltage growth compared to sulphuric acid at the same current density. The sample anodized in $K_2SO_4$ 0.5 M at 10 mA/cm$^2$ required the same time to reach

120 V that the one anodized at 15 mA/cm$^2$ in $H_2SO_4$ 0.5 M. However, curve shapes differ, potassium sulphate showed deviation from linearity at higher voltage, leading to a slower growth below 90 V and faster above this value. The same trend is observed at lower voltages and current densities. Fig. 3 shows galvanostatic anodization at 1 mA/cm$^2$ in $K_2SO_4$ 0.5 M and $H_2SO_4$ 0.5 M, potassium sulphate promoted faster anodization and deviated from linearity at voltages 1 V higher than sulfuric acid.

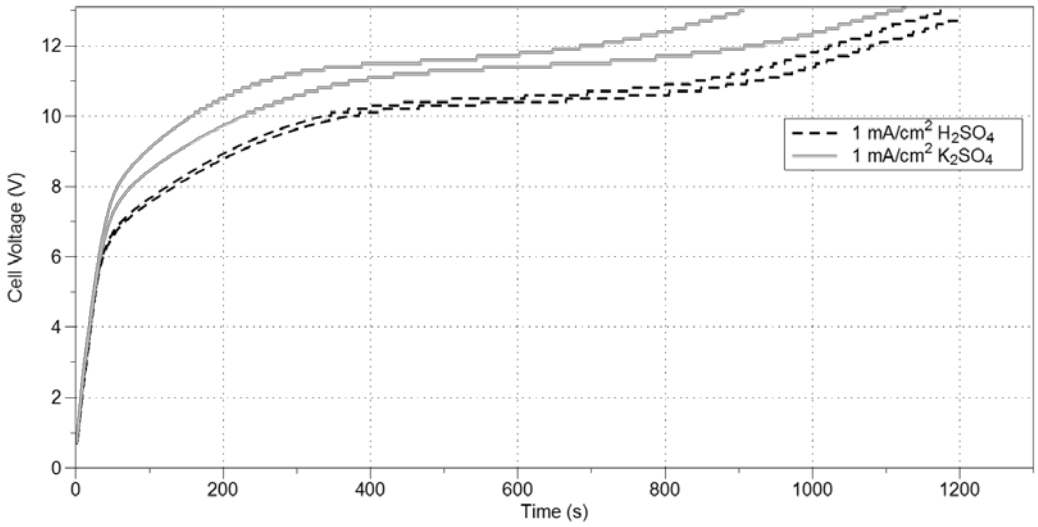


**Figure 3: Cell voltage growth kinetic during galvanostatic anodization in $H_2SO_4$ and $K_2SO_4$ 1 mA/cm$^2$.**

**Anodization efficiency**

Anodization efficiencies at different current densities was obtained as described in Eq. I. Results are plotted in Fig. 4, against cell voltage. All the conditions tested operates at 100 % of efficiency up to a certain voltage, that increases as anodization current density increases. Anodization tests at 5 mA/cm$^2$ kept 100 % until 15 V was reached, while anodization at 20 mA/cm$^2$ reached 35 V before efficiency started to decrease. However, a plateau in efficiency is reached at current density lower than 20 mA/cm$^2$ and this plateau is higher at lower current densities.

The effect of $K_2SO_4$ 0.5 M, compared to $H_2SO_4$ 0.5 M, is to increase the voltage at which efficiency starts to decrease and to reach 120 V at lower efficiency. The effect obtained substituting potassium sulfate to sulfuric acid is to obtain the same trend expected for sulfuric acid at higher current density. This is coherent with anodization kinetic observed in Fig. 2.

The same trend is maintained at lower current density and lower final cell voltage. Anodizations carried out in $K_2SO_4$ 0.5 M shows higher efficiency at lower voltage and lower as voltage increases (Fig. 5).

As most of the anodizing time is spent at high voltage, where voltage growth slows down, the efficiency plateau becomes more evident if plotted against time. However, it is important to remember that oxide thickness is proportional to anodizing cell voltage and that the amount of time spent to reach a certain voltage has a negligible effect on the corresponding oxide growth. In Fig. 6, efficiency evolution with time is shown for anodization carried out at different current densities, in the two considered electrolytes.

Efficiencies, starting from 100 %, after about 100 s decreased to a level that is maintained until anodization regime changes from standard to anodic spark deposition, with consequent dielectric breakdown of the oxide. Anodizations carried out at 20 mA/cm$^2$ reached anodic spark deposition before 100 s, so no plateau is observed. In the other cases, the established plateau value decreased as anodizing current density increases.

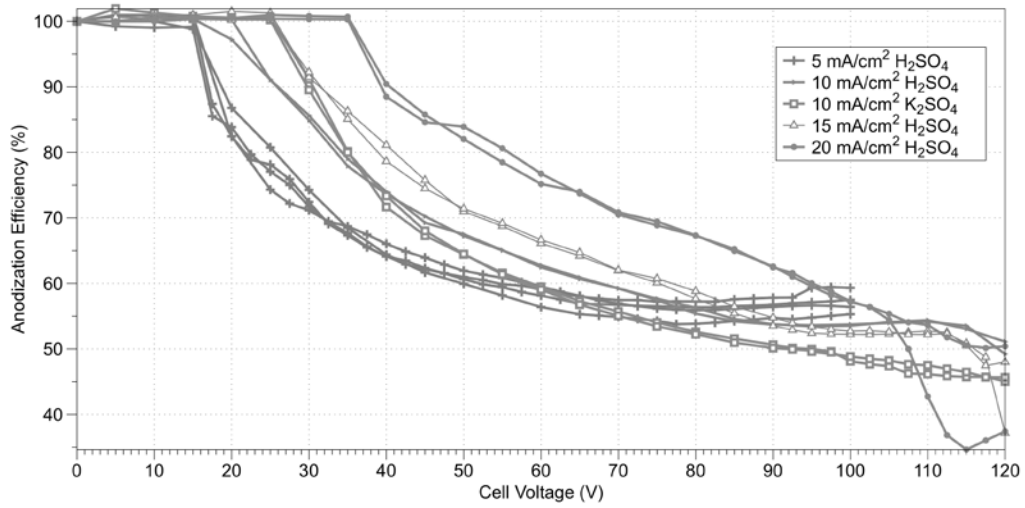


**Figure 4: Anodizing efficiency vs cell voltage reached at different current densities and different electrolytes.**

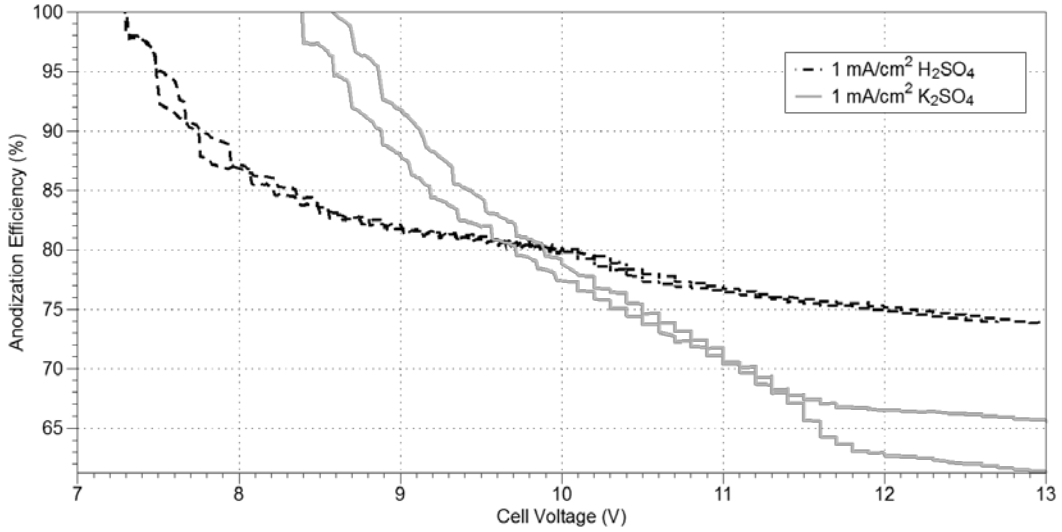


**Figure 5: Anodizing efficiency vs cell voltage during anodization at 1 mA/cm$^2$ in different electrolytes.**

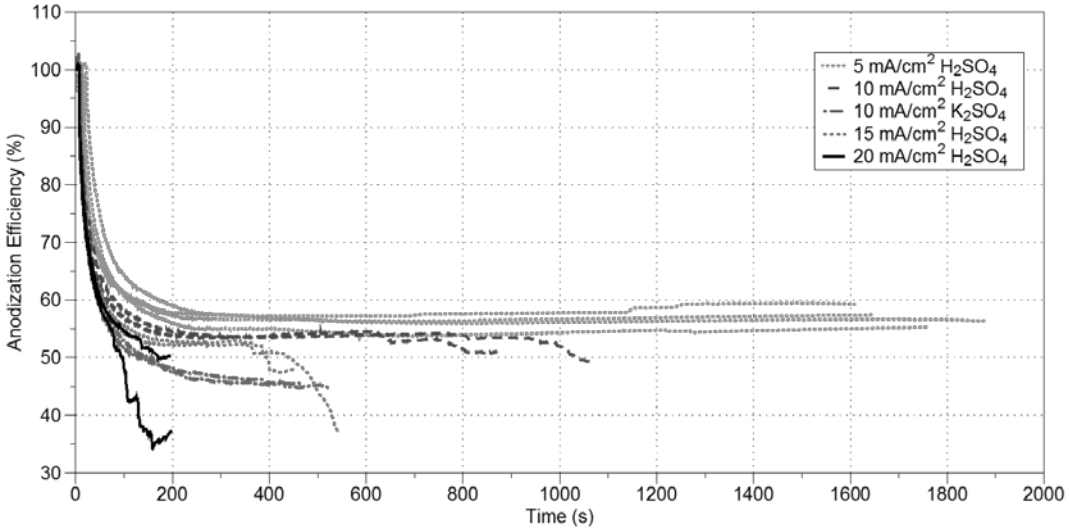


**Figure 6: Anodizing efficiency vs time during anodization in different current densities and different electrolytes.**

### Oxide thickness

In Fig. 4 and Fig. 5 efficiency was considered against final cell voltage. However, comparison between different electrolytes are subjected to the hypothesis that the same cell voltage corresponds to the same oxide thickness. To confirm this hypothesis, anodizations were carried out at voltages ranging from 10 V to 120 V. One series using $H_2SO_4$ 0.5 M and two using $K_2SO_4$ 0.5 M to ensure repeatability. Results are visible in Fig. 7.

Up to 90 V, thicknesses of oxides produced in the two electrolytes are the same. From 90 V results starts to diverge. This is due to the transition to anodic spark deposition regime, in which more oxygen is developed, and the phenomenon becomes less controlled, with a physiological decrease of reproducibility.

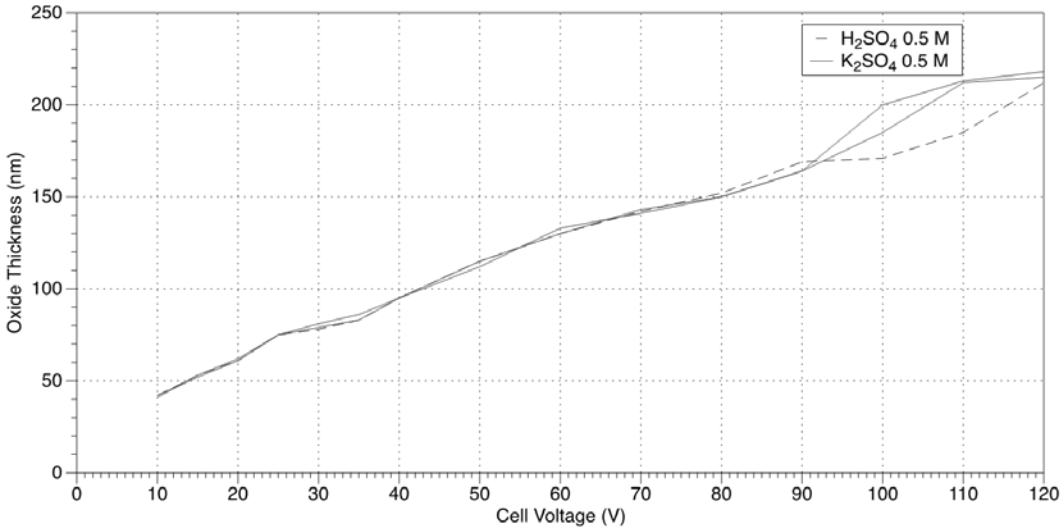


**Figure 7: Thickness of titanium oxide obtained with anodization in $H_2SO_4$ 0.5 M and $K_2SO_4$ 0.5 M at different cell voltages from 10 V to 120 V.**

Oxide film thickness was also used to calculate oxide volume influence on gravimetric setup measurement. Oxide grown at metal surface changes sample volume and weight, leading to possible errors during $O_2$ evolution measurement.

As Pilling-Bedworth ratio for titanium is 1.73, a 220 nm oxide, maximum thickness obtain by spectrophotometric measurements, corresponds to 127 nm of metal oxidized to $TiO_2$. The remaining 93 nm of oxide, on 4 $cm^2$ sample, leads to an increase in volume of $3.72 \cdot 10^{-5}$ $cm^3$ with density 3.7 $g/cm^3$. As electrolyte density is 1.022 $g/cm^3$, the volume in excess caused an error of $9.9 \cdot 10^{-5}$ g during the whole experiment. The error is comparable with setup experimental error, so it was considered negligible.

## DISCUSSION

### Oxygen Evolution interpolated efficiency

By plotting $O_2$ evolution in time (Fig. 8), the linear trend of oxygen evolution is clearly visible. The linearity starts from the first non-zero value and it is loosed at times corresponding to the achievement of cell voltages around 100 V, where anodic spark deposition begins. As the first non-zero measurement appeared after about ten second from experiment beginning, regardless to current density used, this phenomenon is ascribed to the existence of a sort of inertia characteristic of the experimental setup used. The effect of this inertia is to associate an efficiency of 100 % to the first seconds of anodization. This affects the cumulative efficiency of the experiment until the amount of data collected are enough to hide the initial error. This is coherent with the characteristic time necessary to the efficiency to reach a plateau. The slope of $O_2$ evolution associated charge against time, which is the current spent in oxygen evolution parasitic reaction, is more reliable measurement of process efficiency.

The efficiencies calculated using linear fitting of Fig. 8 plot are shown in Table 1 together with cell voltage value at which the plot deviates from linearity.

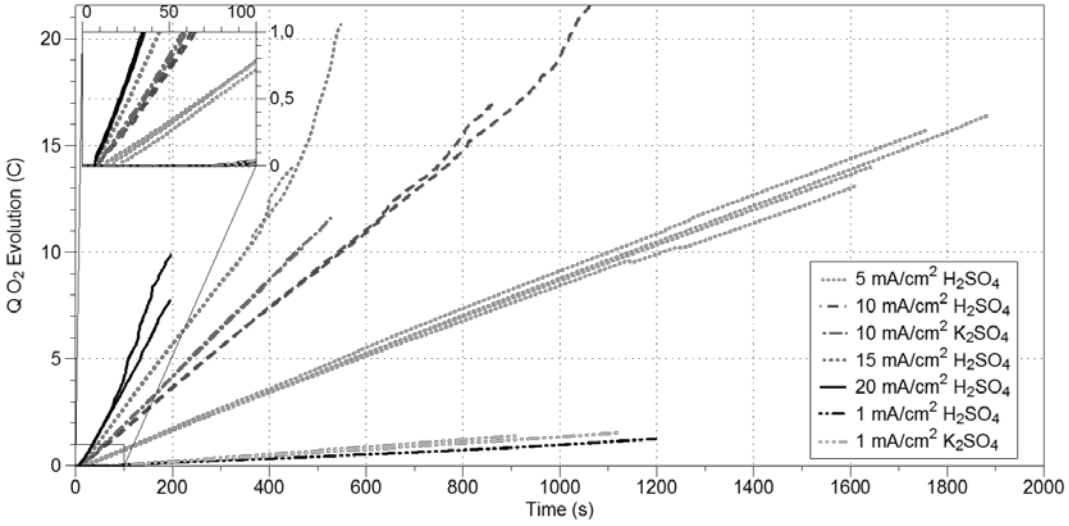


**Figure 8: Charge associated with $O_2$ evolution vs time during anodization at different current densities and in different electrolytes.**

**Table 1**

**Anodizing efficiencies calculated by plotting charge associated with oxygen evolution against time and ranges of linearity.**

| Electrolyte | Anodizing current density (mA/cm$^2$) | $O_2$ evolution current density (mA/cm$^2$) | Efficiency (%) | Diverging voltage (V) |
|---|---|---|---|---|
| $H_2SO_4$ | 20 | 10.5 | 47.6 | 107.5 |
| | 20 | 10.6 | 47.0 | No |
| | 15 | 7.28 | 51.5 | 110 |
| | 15 | 7.39 | 50.7 | 110 |
| | 10 | 4.68 | 53.2 | 115 |
| | 10 | 4.68 | 53.2 | 115 |
| | 5 | 2.26 | 54.8 | No |
| | 5 | 2.19 | 56.3 | No |
| | 5 | 2.14 | 57.1 | No |
| | 5 | 2.03 | 59.4 | No |
| | 1 | 0.263 | 73.7 | No |
| | 1 | 0.264 | 73.6 | No |
| $K_2SO_4$ | 10 | 5.67 | 43.3 | No |
| | 10 | 5.59 | 44.1 | No |
| | 1 | 0.365 | 63.5 | No |
| | 1 | 0.413 | 58.7 | No |

Efficiency remained constant during the whole anodization treatment until anodic spark deposition regime is established. In standard anodization condition it is possible to compare efficiency obtained at different current density, regardless to the anodizing cell voltage. Anodization efficiency increased as current density was decreased, passing from 47 % at 20 mA/cm$^2$ to 73 % at 1 mA/cm$^{2.}$ The same trend is observed both in $H_2SO_4$ 0.5 M and $K_2SO_4$ 0.5 M. Moreover, $O_2$ evolution current density deviation from linearity followed the same trend, happening at higher voltage when current density is decreased.

## CONCLUSIONS

- Galvanostatic anodization kinetic was studied in $H_2SO_4$ 0.5 M at current densities from 1 to 20 mA/cm$^2$ and compared with $K_2SO_4$ 0.5 M. Potassium sulphate leaded to faster anodization compared to sulphuric acid at the same current density.
- Anodization efficiency was studied with live $O_2$ evolution measurement through gravimetric setup. Lower current densities leaded to higher efficiency, that remained constant up to anodic spark deposition regime establishment. Potassium sulphate showed lower efficiency compared to sulphuric acid.
- $O_2$ evolution current density deviates from linearity at higher cell voltages as anodization current density is decreased

## REFERENCES


1. Prando, D., A. Brenna, M.V. Diamanti, S. Beretta, F. Bolzoni, M. Ormellese, and M. Pedeferri, *Journal of Applied Biomaterials & Functional Materials* 15 (2017).
2. Banerjee, D., and J. Williams, *Acta Materialia* 61 (2013): pp. 844–879.
3. Donachie, M.J., *Titanium: A Technical Guide, 2nd Edition* (ASM International, 2000).
4. Alfantazi, A., E. Asselin, and J. Liu, “The Pitting Corrosion of Titanium in Aggressive Environments: A Review” (2016).
5. Deng, B., Y. Jiang, J. Gong, C. Zhong, J. Gao, and J. Li, *Electrochimica Acta* 53 (2008): pp. 5220–5225.
6. Boyer, R.R., *Materials Science and Engineering: A* 213 (1996): pp. 103–114.
7. Chang, S.Y., H.K. Lin, L.C. Tsao, W.T. Huang, and Y.T. Huang, *Corrosion Engineering, Science and Technology* 49 (2014): pp. 17–22.
8. Eylon, D., *Titanium for Energy and Industrial Applications* (Metallurgical Society of AIME, 1981).
9. Froes, F.H., D. Eylon, and H.B. Bomberger, *Titanium Technology: Present Status and Future Trends* (Titanium Development Association, 1985).
10. Virtanen, S., *Corrosion Reviews* 26 (2008): pp. 147–172.
11. Gorynin, I.V., *Materials Science and Engineering: A* 263 (1999): pp. 112–116.
12. Griess, J.C., *Corrosion* 24 (1968): pp. 96–109.
13. Liu, J., A. Alfantazi, and E. Asselin, *Corrosion* 70 (2014): pp. 29–37.
14. Shoesmith, D.W., D. Hardie, B.M. Ikeda, and J.J. Noel, “Hydrogen Absorption and the Lifetime Performance of Titanium Nuclear Waste Containers” (Atomic Energy of Canada Limited, 1997).
15. Prando, D., A. Brenna, M.V. Diamanti, S. Beretta, F. Bolzoni, M. Ormellese, and M. Pedeferri, *Journal of Applied Biomaterials & Functional Materials* 16 (2018): pp. 3–13.
16. Schutz, R.W., *Corrosion of Titanium and Titanium Alloys, Corrosion: Materials* (ASM International, 2005).
17. Beck, T.R., *Journal of the Electrochemical Society* 120 (1973): pp. 1317–1324.
18. Prando, D., Nicolis D., M. Pedeferri, and M. Ormellese, *Materials and Corrosion* 1 (2018).
19. Handzlik, P., and K. Fitzner, *Transactions of Nonferrous Metals Society of China* 23 (2013): pp. 866–875.
20. Neto, G.C.L.B., M.A.M. da Silva, and J. C. Alves, *Surface Engineering* 25 (2009): pp. 146–150.
21. Sathish, S., M. Geetha, N.D. Pandey, C. Richard, and R. Asokamani, *Materials Science and Engineering: C* 30 (2010): pp. 376–382.
22. Vetrivendan, E., J. Jayaraj, S. Ningshen, C. Mallika, and M. Kamachi, *Journal of Thermal Spray Technology* 27 (2018): pp. 512–523.
23. Prando, D., A. Brenna, M. Pedeferri, and M. Ormellese, *Materials and Corrosion* 69 (2017): pp. 503–509.
24. Laube, M., F. Rauch, C. Ottermann, O. Anderson, and K. Bange, *Nuclear Instruments and Methods in Physics Research Section B: Beam Interactions with Materials and Atoms* 113 (1996): pp. 288–292.

25. Valota, A., D. J Leclere, T. Hashimoto, P. Skeldon, G. Thompson, S. Berger, J. Kunze-Liebhäuser, and P. Schmuki, *Nanotechnology* 19 (2008): p. 355701.
26. Delplancke, J.-L., and R. Winand, *Electrochimica Acta* 33 (1988): pp. 1551–1559.
27. Curioni, M., F. Sceinini, T. Monetta, and F. Bellucci, “Investigation of Hydrogen Evolution Behaviour on Corroding Magnesium Electrodes by Electrochemical Impedance Spectroscopy, Real-Time Hydrogen Measurement and Optical Imaging” (2015), p. 1005.
28. Torrescano-Alvarez, J.M., M. Curioni, and P. Skeldon, *Journal of the Electrochemical Society* 164 (2017): pp. C728–C734.
29. Fajardo, S., and G.S. Frankel, *Journal of the Electrochemical Society* 162 (2015): pp. C693–C701.